AD-A077 523 PENNSYLVANIA STATE UNIV UNIVERSITY PARK APPLIED RESE--ETC F/G 11/9
TURBULENCE IN DRAG REDUCING POLYMER SOLUTIONS.(U)
APR 79 I KUBO N00024-79-C-6043
UNCLASSIFIED ARL/PSU/TM-79-66 NL

1 OF 1
ADA 077523

END
DATE FILMED
1-80
DDC

TURBULENCE IN DRAG REDUCING POLYMER SOLUTIONS

I. Kubo

Technical Memorandum
File No. TM 79-66
April 16, 1979
Contract No. N00024-79-C-6043

Copy No. 41

The Pennsylvania State University
APPLIED RESEARCH LABORATORY
Post Office Box 30
State College, PA 16801

NAVY DEPARTMENT

NAVAL SEA SYSTEMS COMMAND

UNCLASSIFIED

SECURITY CLASSIFICATION OF THIS PAGE (When Data Entered)

REPORT DOCUMENTATION PAGE	READ INSTRUCTIONS BEFORE COMPLETING FORM
1. REPORT NUMBER: TM 79-66	2. GOVT ACCESSION NO.	3. RECIPIENT'S CATALOG NUMBER: (9)
4. TITLE (and Subtitle): (6) TURBULENCE IN DRAG REDUCING POLYMER SOLUTIONS.	5. TYPE OF REPORT & PERIOD COVERED: Technical Memorandum (13)
	6. PERFORMING ORG. REPORT NUMBER
7. AUTHOR(s): (10) I. Kubo	8. CONTRACT OR GRANT NUMBER(s): (15) N00024-79-C-6043
9. PERFORMING ORGANIZATION NAME AND ADDRESS: Applied Research Laboratory, P. O. Box 30, State College, PA 16801	10. PROGRAM ELEMENT, PROJECT, TASK AREA & WORK UNIT NUMBERS: (12) 35
11. CONTROLLING OFFICE NAME AND ADDRESS: Naval Sea Systems Command, Code 63R-31, Washington, DC 20362	12. REPORT DATE: (11) 16 Apr 79
	13. NUMBER OF PAGES: 28
14. MONITORING AGENCY NAME & ADDRESS (if different from Controlling Office): (14) ARL/PSU/TM-79-66	15. SECURITY CLASS. (of this report): UNCLASSIFIED
	15a. DECLASSIFICATION/DOWNGRADING SCHEDULE

16. DISTRIBUTION STATEMENT (of this Report)

Approved for Public Release. Distribution Unlimited.
Per NAVSEA - August 30, 1979.

17. DISTRIBUTION STATEMENT (of the abstract entered in Block 20, if different from Report)

18. SUPPLEMENTARY NOTES

Presented at Sixth Biennial Symposium on Turbulence, October 8-10, 1979, University of Missouri - Rolla, and to be published in the proceedings of the meeting.

19. KEY WORDS (Continue on reverse side if necessary and identify by block number)

20. ABSTRACT (Continue on reverse side if necessary and identify by block number)

Measurements were made of the mean and fluctuating velocity profile with a Laser Doppler Velocimeter in a fully developed turbulent pipe flow of a polymer drag reducing solution. A one-equation turbulence model has been developed by using a damping factor similar to that of Mizushima and Usui. Predictions by the model agree well with experimental data for the mean velocity profile and for the increase of the length scale in polymer solutions. Predictions are also compatible with the streamwise turbulent

DD FORM 1 JAN 73 1473 EDITION OF 1 NOV 65 IS OBSOLETE

UNCLASSIFIED 391 007

SECURITY CLASSIFICATION OF THIS PAGE (When Data Entered)

intensity measurements and show similar trends to the measured intensity distributions in Newtonian fluids and polymer solutions. In highly reduced drag region, predictions, together with the measurements, indicate considerable effect of Reynolds number below Re = 4×10^4 (40,000) on the turbulent intensity profile.

Subject: Turbulence in Drag Reducing Polymer Solutions

References: See Page 17

Abstract: Measurements were made of the mean and fluctuating velocity profile with a Laser Doppler Velocimeter in a fully developed turbulent pipe flow of a polymer drag reducing solution. A one-equation turbulence model has been developed by using a damping factor similar to that of Mizushima and Usui. Predictions by the model agree well with experimental data for the mean velocity profile and for the increase of the length scale in polymer solutions. Predictions are also compatible with the streamwise turbulent intensity measurements and show similar trends to the measured intensity distributions in Newtonian fluids and polymer solutions. In highly reduced drag region, predictions, together with the measurements, indicate considerable effect of Reynolds number below $Re = 4 \times 10^4$ on the turbulent intensity profile.

Acknowledgments: The author wishes to express his appreciation to Drs. J. L. Lumley, G. H. Hoffman, and H. Usui for their helpful advice. Particular credit is due Dr. G. H. Hoffman for suggesting a number of useful avenues during this investigation. This research was supported by the U. S. Naval Sea Systems Command, Code NSEA 63R-31.

Table of Contents

List of Figures

I. INTRODUCTION

Considerable progress has been made in recent years toward the understanding of wall-bounded turbulent shear flows in Newtonian fluids,[1] whereas the same cannot be said for the same type of polymer flows which are of considerable interest because of the drag reduction phenomenon. Some measurements on the mean and fluctuating velocity profiles and of the large scale structure in turbulent polymer flows are available and are discussed in a recent review by Berman.[2] Measured mean velocity profiles among investigators[3,4,5] agree in several aspects and general features of the profile have begun to emerge. In the laminar sublayer region, the velocity profile obeys $u^+ = y^+$, as a Newtonian fluid. A change in the velocity profile is observed in the buffer layer which extends into the logarithmic region. At the maximum drag reduction point, the logarithmic region disappears. Concerning the turbulent intensity profiles, the few available experimental data[4,5,6] all conflict on the magnitude of the peak intensity. Rudd,[6] using a pipe with a square cross section, observed a large increase in the axial intensity distribution for a polymer solution whereas no other experimental measurements of polymer flows in channels and circular pipes show such a large increase. Measurements by Mizushima and Usui[5] and Reischman and Tiederman[4] are closer to each other than to the data of Rudd[6]. Yet they disagree on whether the peak intensity is higher in a polymer

solution than in a Newtonian fluid. In this paper, a one-equation turbulence model is developed and, together with some experimental measurements, an attempt is made to study the general features of turbulence in polymer solutions. An explanation for the conflict between the two turbulence measurements[4,5] in polymer solutions is offered.

II. EXPERIMENTS

The pipe flow facility used in the present experiment and a detailed view of the test section are shown in Figure 1. The straight inlet pipe length is approximately 160-pipe diameters. The pressure drop was measured by a ultra low range differential pressure transducer over a 75-inch length across the test section. Linearity of the pressure drop in the inlet section of the pipe was checked for both solvent and polymer solutions. For velocity measurements, a Laser Doppler Velocimeter was employed. The measuring section of the pipe is constructed with a thin polyester film (51 μm thick) similar to that of Mizushima and Usui.[5] This construction enables velocity to be measured close to the pipe wall and the smallest dimension of the measuring volume to be aligned in the direction of the steepest velocity gradient, minimizing the velocity biasing[7] and the broadening of Doppler signals due to the velocity gradient.[8] With the analysis of laminar flow measurements, the measuring volume was found to be about 0.05 x 0.05 x 0.250 (mm^3), and the error due to the finite transit time broadening was less than 2.2 percent.

The polymer used was polyethylenoxide (Union Carbide WSR-301) with an intrinsic viscosity measured to be 12.5 dl/g. The flow rate was measured with a precision flow meter which was calibrated for both water and polymer solutions prior to the experiment by using a weighing scale and a stop watch. At present, due to the capacity of this meter, the highest Reynolds number, based on the pipe diameter, achievable for the experiments was limited to around 12,000.

III. TURBULENCE MODEL AND THE GOVERNING EQUATIONS

Because of the success of the algebraic turbulence model of Mizushima and Usui[5] applied to flows with drag reduction, a simple one-equation turbulence model which prescribes the length scale and considers the transport of turbulent kinetic energy was developed. The model is a modification of the Hassid and Poreh[9] scheme by adopting the Mizushima and Usui[5] damping factor and by modifying the dissipation term to account the polymer effects in the buffer zone. The eddy diffusivity is expressed by

$$\varepsilon = C_\mu k^{\frac{1}{2}} L \left\{ 1 - \exp \left[- A_\mu R_t \left(-\alpha + (\alpha^2 + l_1)^{\frac{1}{2}} \right)^{\frac{1}{2}} \right] \right\} . \qquad (1)$$

The damping factor is similar to the form used by Mizushima and Usui,[5] except that the Van Driest constant, A_+, and y_+ are replaced by the constant, A_μ, and the Reynolds number of turbulence, R_t:

$$R_t = \frac{k^{\frac{1}{2}} L}{\nu} , \qquad (2)$$

since the Van Driest mixing length model is found to give unsatisfactory results for low Reynolds number flows. The value of α is determined in exactly the same way as Mizushima and Usui,[5] namely,

$$\alpha = \left(\frac{2\lambda}{\nu}\right)\left(\frac{U_*}{26}\right)^2 \quad , \tag{3}$$

where λ, ν, U_* are the relaxation time for the Maxwell model, the kinematic viscosity and the friction velocity, respectively. The constant λ is determined from the relaxation time for simple laminar shear flow, λ_ℓ, as

$$\frac{\lambda}{\lambda_\ell} = 3.76 \times 10^8 \, W^{1.34} \quad , \tag{4}$$

where W is the Weisenberg number $= \lambda_\ell \, \overline{U}/2R$, $\overline{U}$ is the mean velocity and R is radius of the tube. The calculation of λ_ℓ was performed using the equation derived by James and Acosta.[10] All coefficients used to determine α had the same values as those used by Mizushima and Usui.[5]

The length scale, L, is prescribed by using Nikuradse's relation:

$$L = y\left[1 - 1.1\left(\frac{y}{R}\right) + 0.6\left(\frac{y}{R}\right)^2 - 0.15\left(\frac{y}{R}\right)^3\right] \quad . \tag{5}$$

Then the turbulent energy is obtained by solving the transport equation:

$$\frac{Dk}{Dt} = \frac{\partial}{\partial x_j}\left[\nu\frac{\partial k}{\partial x_j} - \overline{u_j\left(\frac{p}{\rho} + \frac{u_i}{2}\right)^2}\right] - \overline{u_i u_j}\frac{\partial U_i}{\partial x_j} - \overline{\nu\left(\frac{\partial u_i}{\partial x_j}\right)^2} \quad , \tag{6}$$

together with the following assumptions:

$$\overline{-u_j\left(\frac{p}{\rho}+\frac{u_i^2}{2}\right)} = \frac{\varepsilon}{\sigma_k}\frac{\partial k}{\partial x_j} \quad , \tag{7}$$

and

$$\nu\overline{\left(\frac{\partial u_i}{\partial x_j}\right)^2} \equiv \Delta = \frac{2\nu k}{L^2} + \frac{C_D k^{3/2}}{L}\left\{1 - \exp\left[-A_\mu R_t \Big/ \left(-\alpha + (\alpha^2+1)^{\frac{1}{2}}\right)^{\frac{1}{2}}\right]\right\} \quad . \tag{8}$$

In the region close to the wall, viscous diffusion is balanced by viscous dissipation and the turbulent kinetic energy varies as y^2. The first term in Equation (8) is introduced to satisfy these two conditions simultaneously, since the second term alone cannot satisfy them. Jones and Launder[11] used $2\nu(\partial k^{\frac{1}{2}}/\partial y)^2$ instead of $2\nu k/L^2$. The results should not differ much because this term is only important near the wall and the distribution of $k^{\frac{1}{2}}$ is nearly linear in that region. Physically, this term is interpreted as the dissipation due to the large eddies which partially submerge in the viscous sublayer (Townsend).[12] Lumley's[13] explanation is that the eddy being parasitic does not contribute to the Reynolds stress and that its size and intensity are determined by the mean velocity profile. Since its scale is much larger than the polymer molecules and it loses energy mainly in the viscous sublayer region where polymer molecules are not stretched, the dissipation due to the large eddy will not be affected by polymer concentration.

The second term of Equation (8) is considered to be the dissipation due to small eddies through the energy "cascade" process. At high

turbulent Reynolds numbers, dissipation is mainly due to the small eddies and large eddy dissipation is almost negligible. At the buffer zone, however, the turbulent Reynolds number is not large so that turbulent energy is dissipated even in the smaller wave number region. Therefore, for Newtonian fluids ($\alpha = 0$), a damping factor $\{1 - \exp(-A_\mu R_t)\}$, is multiplied to the usual $C_D k^{3/2}/L$ term. In polymer solutions, polymer molecules are stretched in the buffer zone and the stretched polymer molecule size is comparable to the Kolmogorov microscale. Justification for the term $\left(-\alpha + (\alpha^2 + 1)^{\frac{1}{2}}\right)^{\frac{1}{2}}$ in the damping factor of the dissipation term is that, due to the polymer, the proportion of the two types of dissipation will change.

The model constants C_μ and C_D are the same as those of Wolfstein[14] who determined them from the conditions in the vicinity of the wall where convection and diffusion of energy are negligible. The value of α is obtained from Equations (3) and (4), exactly in the same way as Mizushima and Usui.[5] The sets of constants used here are the same as those of Hassid and Poreh,[9] summarized as follows:

$$C_\mu = 0.416, \qquad C_D = 0.22,$$
$$A_\mu = 0.012, \qquad \sigma_k = 1.0 \quad . \tag{9}$$

The turbulent-energy equation model for polymer solutions developed here was applied to fully developed turbulent pipe flow. In dimensionless, universal variables, the governing equations are:

$$(1 + \varepsilon_+) \frac{dU_+}{dy_+} = \left(1 - \frac{y_+}{R_+}\right) \quad , \tag{10}$$

$$\varepsilon_+ = C_\mu k_+^{\frac{1}{2}} L_+ \left\{ 1 - \exp\left[- A_\mu k_+^{\frac{1}{2}} L_+ \left(- \alpha + (\alpha^2 + 1)^{\frac{1}{2}} \right)^{\frac{1}{2}} \right] \right\} \quad , \qquad (11)$$

$$L_+ = y_+ \left[1 - 1.1 \left(\frac{y_+}{R_+} \right) + 0.6 \left(\frac{y_+}{R_+} \right)^2 - 0.15 \left(\frac{y_+}{R_+} \right)^3 \right] \quad , \qquad (12)$$

$$\frac{1}{(R_+ - y_+)} \frac{d}{dy_+} \left[(R_+ - y_+) (1 + \varepsilon_+) \frac{dk_+}{dy_+} \right]$$

$$= \frac{\varepsilon_+ (1 - y_+/R_+)^2}{(1 + \varepsilon_+)^2} - \frac{2k_+}{L_+^2} - \frac{C_D k_+^{3/2}}{L_+} \left\{ 1 - \exp\left[-A_\mu k_+^{\frac{1}{2}} L_+ / \left(- \alpha + (\alpha^2 + 1)^{\frac{1}{2}} \right)^{\frac{1}{2}} \right] \right\} \quad . \qquad (13)$$

Numerical solutions of the resulting equations were obtained by using a second-order accurate finite difference scheme, solved with Gauss-Seidel relaxation. Boundary conditions for the turbulent kinetic energy are:

$$k = 0 \qquad \text{at } y = 0 \qquad (14a)$$

$$k = k_0 + k_1 r^2 \qquad \text{near centerline of pipe} \qquad (14b)$$

where k_1 is a constant obtained from Equations (13) and (14b).

In order to place many grid points near the wall, where the gradients are large, the following transformation is used:

$$\eta = \ell n \, (1 + y_+) \quad . \qquad (15)$$

IV. COMPARISON OF PREDICTION WITH EXPERIMENTAL RESULTS

Mean velocity profiles are shown in Figure 2. For the maximum drag reduction asymptote calculation, the value of α was set equal to 40 following Reference 5. Velocity profiles calculated with the same α change for different Reynolds numbers. The prediction for the maximum drag reduction at a Reynolds number of 14,400 agrees well with the experimental data of a 300 ppm polymer solution by Mizushima and Usui[5] at the same Reynolds number. For the three other comparisons made for polymer solutions the agreement is also good. For each of these cases, the value of α was determined by using Equations (3) and (4), together with U_*, $\overline{U}$, and T obtained from the experiments. All three predicted velocity profiles deviate from $U_+ = y_+$ line at around y_+ of 10. Measured mean velocity profiles in the near-wall region ($y_+ < 25$) obtained by Reischman and Tiederman[4] show the same kind of deviation.

The coefficient of resistance versus Reynolds number is shown in Figure 3. The $\alpha = 0$ predicted curve coincides with Prandtl's curve except in the very low Reynolds number range and, as can be seen, the present experimental data are in excellent agreement with the calculations. Various calculations made for different values of α are also shown. The maximum asymptote predicted with $\alpha = 40$ differs slightly and has a slightly flatter profile compared with that of Mizushima and Usui.[5] Points A, B, and C in Figure 3 were obtained from the experiments corresponding to the velocity profiles shown in Figure 2. Values of α shown in Figure 2 for each predicted velocity profile agree well with the values which can be deduced from Figure 3.

Turbulent energy distributions are shown in Figure 4. The predictions by Hassid and Poreh[9] show a large increase in the energy for flows with drag reduction with a maximum value close to that measured by Rudd.[6] Rudd's[6] data were obtained in a one-half inch square duct so that it is highly likely that the data were contaminated with the secondary flow effects of the corners. This is seen from Rudd's[6] measurements for water which indicate significantly higher turbulent intensity than other experimental results (Reischman and Tiederman,[4] Eckelmann and Reichardt,[15] Bakewell,[16] and Pennel, et al.).[17] The present measurements for water are in closer agreement to the latter investigators' results as shown in Figure 5. Present predictions simulate the tendency of the data obtained by Reischman and Tiederman[4] which show a slight increase in the (u_+) peak for a polymer solution with the peak occurring at about $y_+ = 40$. The data of Mizushima and Usui,[5] however, show a decrease in the (u_+) peak. As will be explained later, this may be attributed to the lower Reynolds numbers at which the experiments by Mizushima and Usui[5] were performed.

Both experimental data (References 4 and 5) and present predictions indicate a decline in the turbulent intensity in the region $y_+ \leq 20$. Figure 5 shows the turbulent intensity distribution for different Reynolds numbers. Calculated results indicate the Reynolds number effect is significant for a polymer solution, whereas the effect for the solvent is minimal. The experimental data support this tendency. The turbulent intensity with a Reynolds number of 11,000 is significantly higher than at a Reynolds number of 7,200. The data points (D and E)

correspond to points D and E in Figure 3 and are for high drag reduction conditions. Predicted Reynolds number effect on the peak turbulent intensity and its location are shown in Figure 6, together with the experimental data of Figure 5. For Newtonian fluids, the effect is negligible for a Reynolds number higher than 1×10^4. For flows with large drag reduction, the effect on the peak turbulent intensity is significant for a Reynolds number up to around 5×10^4 and there is a Reynolds number above which the turbulent intensity is higher than that of the solvent and below which the intensity is lower. Experimental data taken at Reynolds numbers of 7,200 and 11,000 follow the same trend as the predictions indicate. On the location of the peak turbulent intensity, on the other hand, the Reynolds number effect is small. The difference of the (u_+) peak for polymer solutions between the data by Mizushima and Usui[5] and that by Reischman and Tiederman[4] may be attributed to the Reynolds number effect, since the former is taken at a Reynolds number range between 9,500 and 35,000 and the latter between 20,000 and 52,000.

The predicted increase in the length scale for a polymer solution is compared with experimental data in Figure 7. Length scale measured in the experiments was the mean spacing between the low speed streaks. A good measure of this spacing should be the thickness of the laminar sublayer. Therefore, a laminar sublayer thickness based on the maximum of the turbulent energy production is used for the prediction. The predicted length scale increase agrees well with the data by Donahue, Tiederman, and Reischman,[18] and by Oldaker and Tiederman.[19]

Figures 8 and 9 show the turbulent energy balance predicted by the model for a Newtonian fluid and for a polymer solution in the maximum drag reduction region ($\alpha = 40$). A significant contrast between the two is that, for a flow with maximum drag reduction, the dissipation due to the second term in Equation (8) is dominant except in the region close to the wall, i.e., $y_+ < 10$, and total dissipation is mainly due to the second term which is defined as an energy cascade type of dissipation. For a Newtonian fluid, the first term in Equation (8), i.e., the dissipation due to the large eddies, plays a significant role in the total dissipation, whereas the second term does not dominate the dissipation until y_+ becomes greater than around 30.

Although the model adopted is extremely simple, a rough qualitative argument may be made on the spectrum of turbulence from Figures 8 and 9. The dissipation associated with the mean velocity gradient is expected to be at relatively low frequency, while the cascade type of dissipation occurs at a relatively high frequency. For a Newtonian fluid, Figure 8 shows that the higher frequency content will increase with the distance from the wall up to $y_+ \doteqdot 30$. The experimental data by Bakewell,[15] which shows the spectra of the streamwise velocity fluctuations at $y_+ = 10$, 20, and 40, confirm this trend (see Figure 10). For polymer solutions, there is no spectral data available. The author has attempted to obtain these data but the small difference in the change of frequency content, as seen in Figure 10, and the spectrum error inherent to the Laser Doppler Velocimeter prevented any definite conclusion from being formed.

Calculation results indicate the cascade type of dissipation dominates polymer flows in the maximum drag reduction region. It should be noted, however, this does not imply that fluctuating velocities in polymer flows have a higher-frequency content than those for a Newtonian fluid. It simply means that in polymer flows the energy is cascaded to small eddies before it dissipates. In fact, the spectral analysis of the fluctuating velocity shows the Newtonian flow contains higher-frequency fluctuation than polymer solutions.

The prediction that the dissipation associated with the cascade dominates in the maximum drag reduction region contradicts the argument by Lumley[13] who predicted the turbulence to consist primarily of large eddies in that region. More experimental investigations are needed to shed light on this point.

V. CONCLUSION

1. Laser Doppler Velocimeter measurements were made of the mean and fluctuating velocity profile in a fully developed turbulent pipe flow of polymer drag reducing solutions.

2. A one-equation turbulence model has been developed, as an extenstion of the Mizushima and Usui[5] algebraic model. The dissipation term in the kinetic energy equation is divided into two terms, i.e., one associated with the changes in wall shear and the other with the energy cascade. The polymer effects are accounted for by changing the proportion of the two types of dissipation.

3. Predictions by the model agree well with experimental data for both mean velocity and turbulence intensity profiles, as well as for the increase of the length scale in the polymer solutions.

4. In the highly reduced drag region, the effect of Reynolds number below $Re = 4 \times 10^4$ on the turbulence structure seems important. Conflicting results between Reischman and Tiederman[4] and Mizushima and Usui[5] over the axial turbulent intensity profile may be attributed to this Reynolds number effect.

5. More experimental investigations, including the study of Reynolds number effects, are needed to clarify the turbulence structure for flows with drag reduction.

REFERENCES

1. Smith, C. R., and Abbott, D. E., (Ed.), An AFOSR/Lehigh University Workshop on Coherent Structure of Turbulent Boundary Layers, Lehigh University, Bethlehem, Pennsylvania, 1978.

2. Berman, N. S., "Drag Reduction by Polymers," Ann. Rev. Fluid Mech., 10, 47, 1978.

3. Virk, P. S., "Drag Reduction Fundamentals," AIChE J., 21, p. 625, 1975.

4. Reischman, M. M., and Tiederman, W. G., "Laser-Doppler Anemometer Measurements in Drag-Reducing Channel Flows," J. Fluid Mech., 70, p. 369, 1975.

5. Mizushima, T., and Usui, H., "Reduction of Eddy Diffusion for Momentum and Heat in Viscoelastic Fluid Flow in a Circular Tube," Phys. Fluids, Supple. 20, p. S100, 1977.

6. Rudd, M. J., "Velocity Measurements Made with a Laser Dopplermeter on the Turbulent Pipe Flow of a Dilute Polymer Solution," J. Fluid Mech., 51, p. 673, 1972.

7. Owen, J. M., and Rogers, R. H., "Velocity Biasing in Laser Doppler Anemometers," Proceedings of the LDA Symposium, Copenhagen, Denmark, p. 89, 1975.

8. Edwards, R. U., Angus, J. C., French, M. J., and Dunning, Jr., J. W., "Spectral Analyses of the Signal from the Laser Doppler Flowmeter: Time-Independent Systems," J. Appl. Phys., 42, p. 837, 1971.

9. Hassid, S., and Poreh, M., "A Turbulent Energy Model for Flows with Drag Reduction," J. Fluids Eng., Trans. ASME, 97, p. 234, 1975.

10. James, D. F., and Acosta, A. J., "The Laminar Flow of Dilute Polymer Solutions Around Circular Cylinders," J. Fluid Mech., 42, p. 269, 1970.

11. Jones, W. P., and Launder, B. E., "The Calculation of Low-Reynolds-Number Phenomena with a Two-Equation Model of Turbulence," Int. J. Heat Transfer, 16, p. 1119, 1973.

12. Townsend., A. A., The Structure of Turbulent Shear Flow, Cambridge University Press, Cambridge, Massachusetts, 1954.

13. Lumley, J. L., "Drag Reduction in Turbulent Flow by Polymer Additives," J. Polymer Sci., 7, p. 263, 1973.

REFERENCES (continued)

14. Wolfstein, M., "The Velocity and Temperature Distribution in One-Dimensional Flow with Turbulence Augmentation and Pressure Gradient," Int. J. Heat Mass Transfer, 12, p. 301, 1969.

15. Eckelman, H., and Reichart, H., "An Experimental Investigation in a Turbulent Channel Flow with a Thick Viscous Sublayer," Proceedings of Turbulence in Liquids Symposium, University of Missouri-Rolla, (Ed. J. L. Zakin and G. K. Patterson), p. 1944, 1971.

16. Bakewell, Jr., H. P., "An Experimental Investigation of the Viscous Sublayer in Turbulent Pipe Flow," Ph.D. Thesis, Department of Aerospace Engineering, The Pennsylvania State University, University Park, Pennsylvania, 1966

17. Pennel, W. T., Sparrow, E. M., and Eckert, E. R. G., "Turbulence Intensity and Time Mean Velocity Distributions in Low Reynolds Number Turbulent Pipe Flows," Int. J. Heat Mass Transfer, 15, p. 1067, 1972.

18. Donohue, G. L., Tiederman, W. G., and Reischman, M. M., "Flow Visualization of the Near-Wall Region in a Drag-Reducing Channel Flow," J. Fluid Mech., 56, p. 559, 1972.

19. Oldaker, D. K., and Tiederman, W. G., "Spatial Structure of the Viscous Sublayer in Drag-Reducing Channel Flows," Phys. Fluids, 20, S133, Part II, 1977.

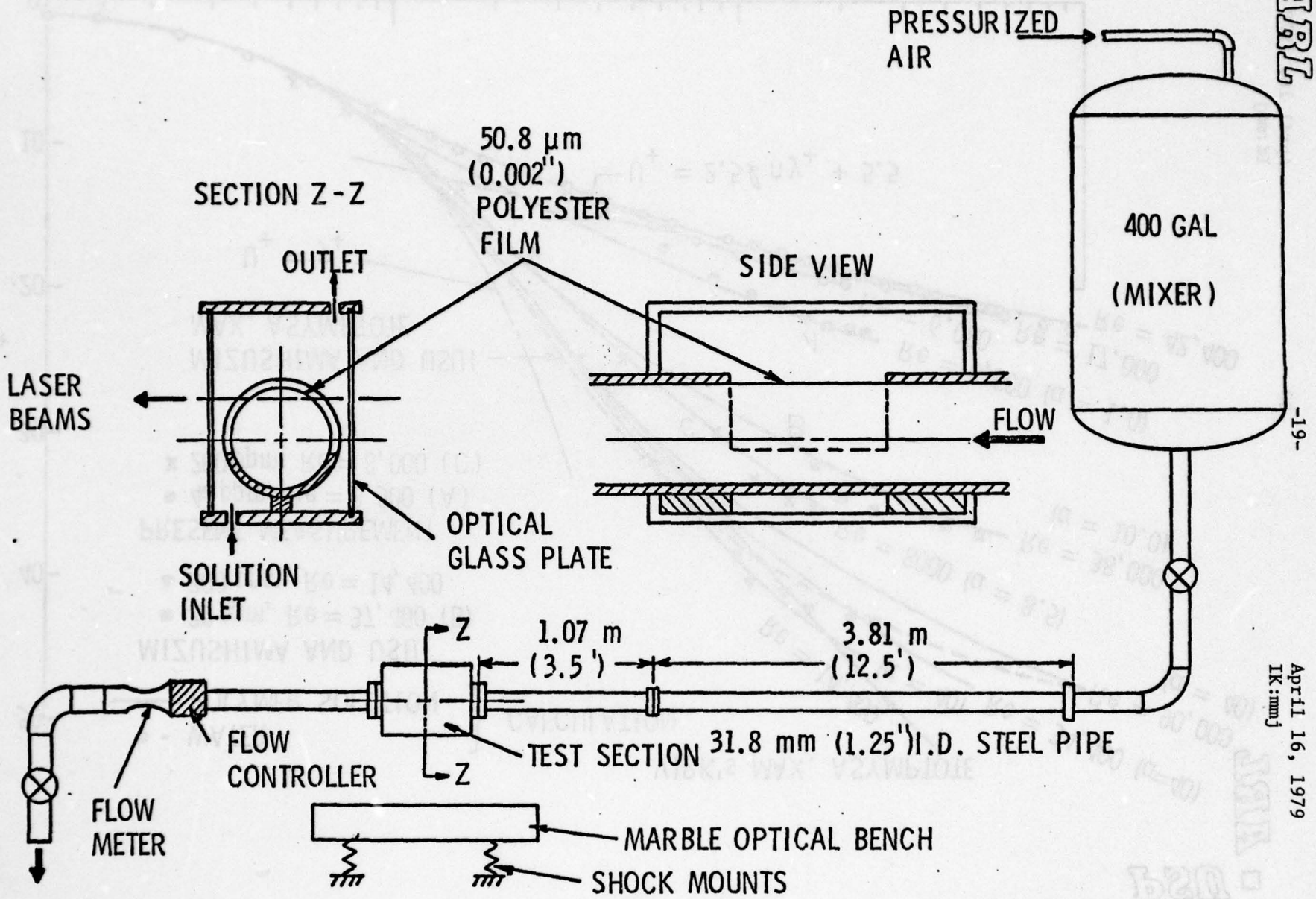

Figure 1. Pipe Flow Facility

April 16, 1979
IK:mmj

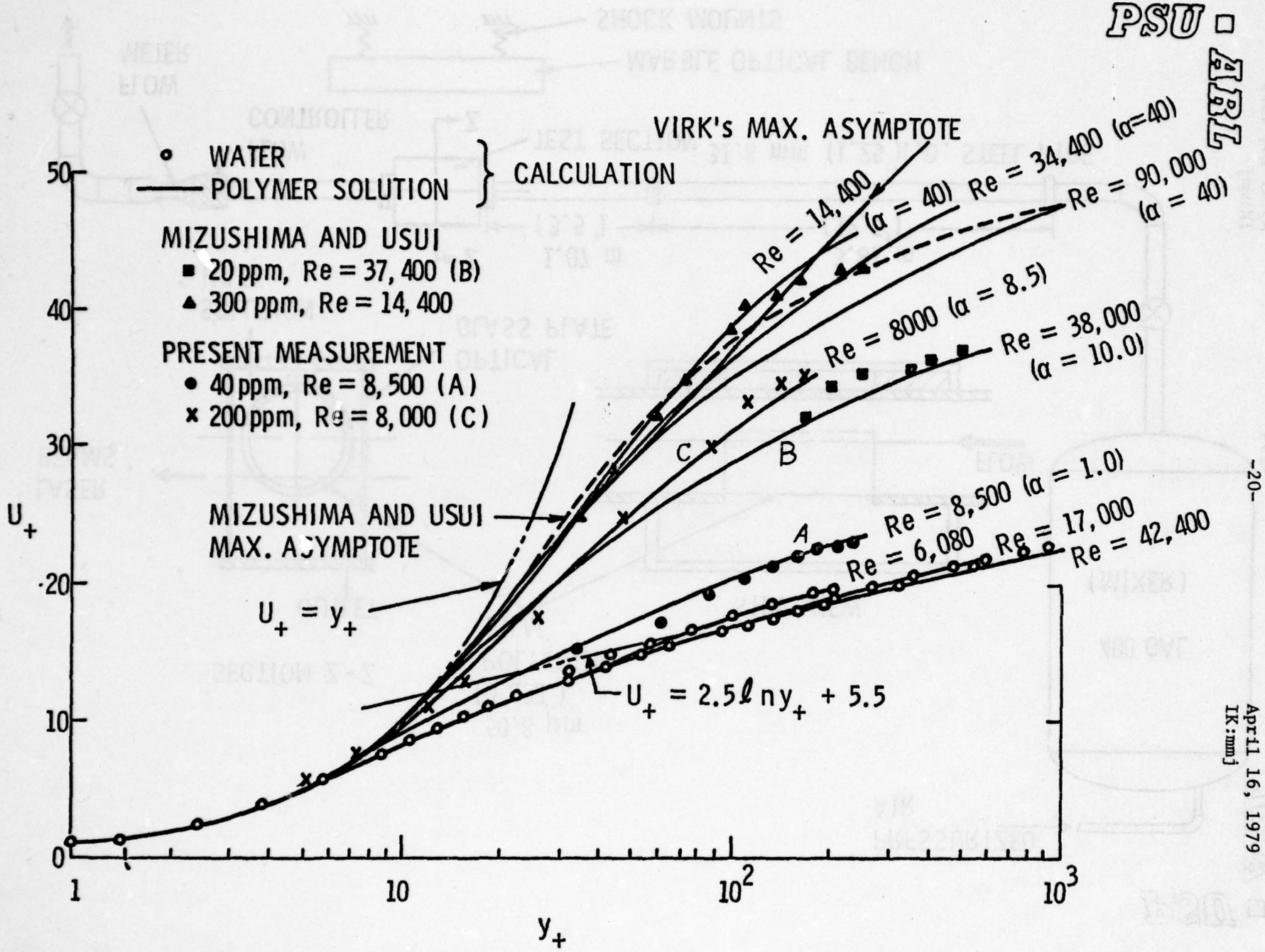

Figure 2. Comparison of Calculated and Measured Mean Velocity

April 16, 1979
IK:mmj

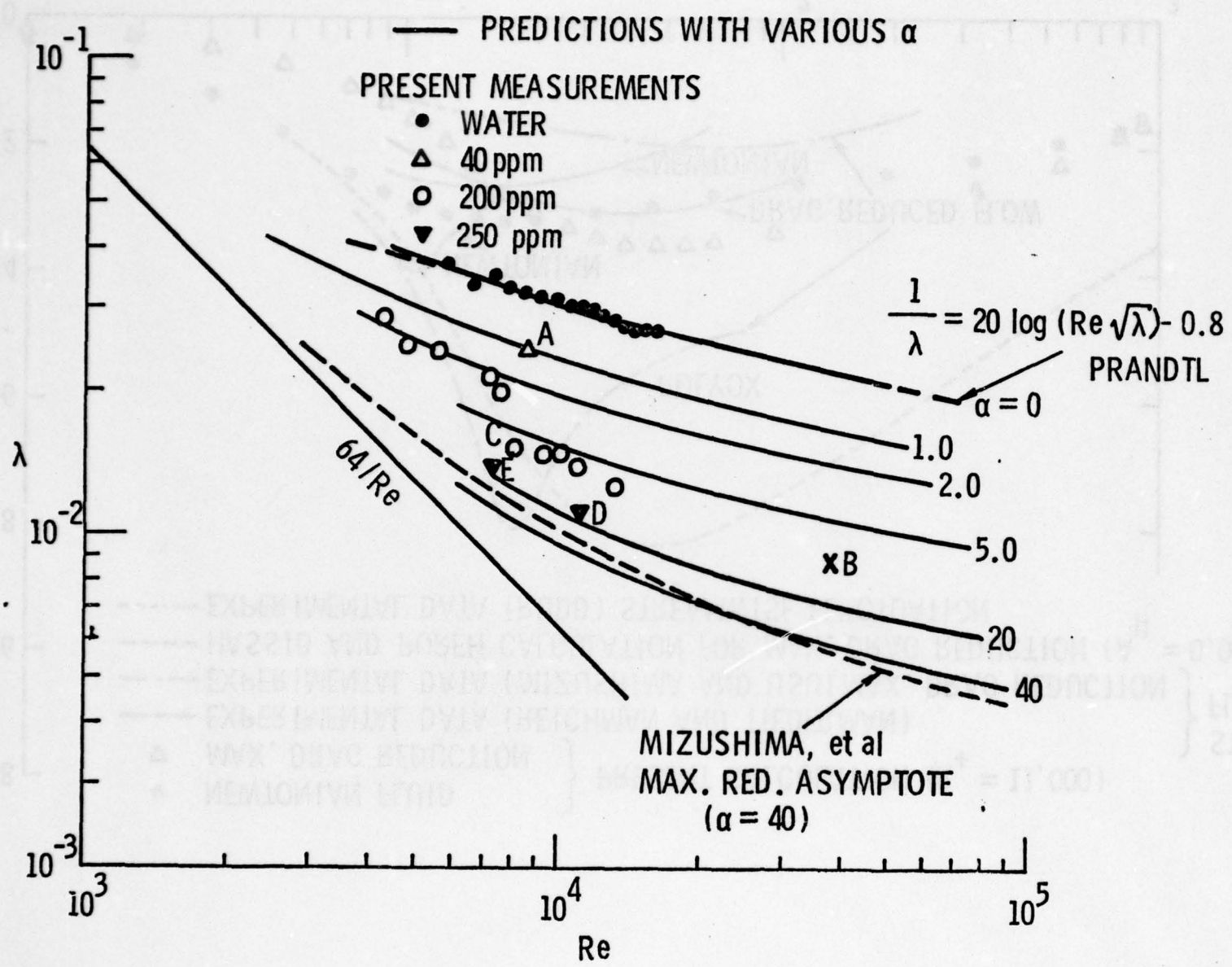

Figure 3. Resistance Coefficient versus Reynolds Number

April 16, 1979
IK:mmj

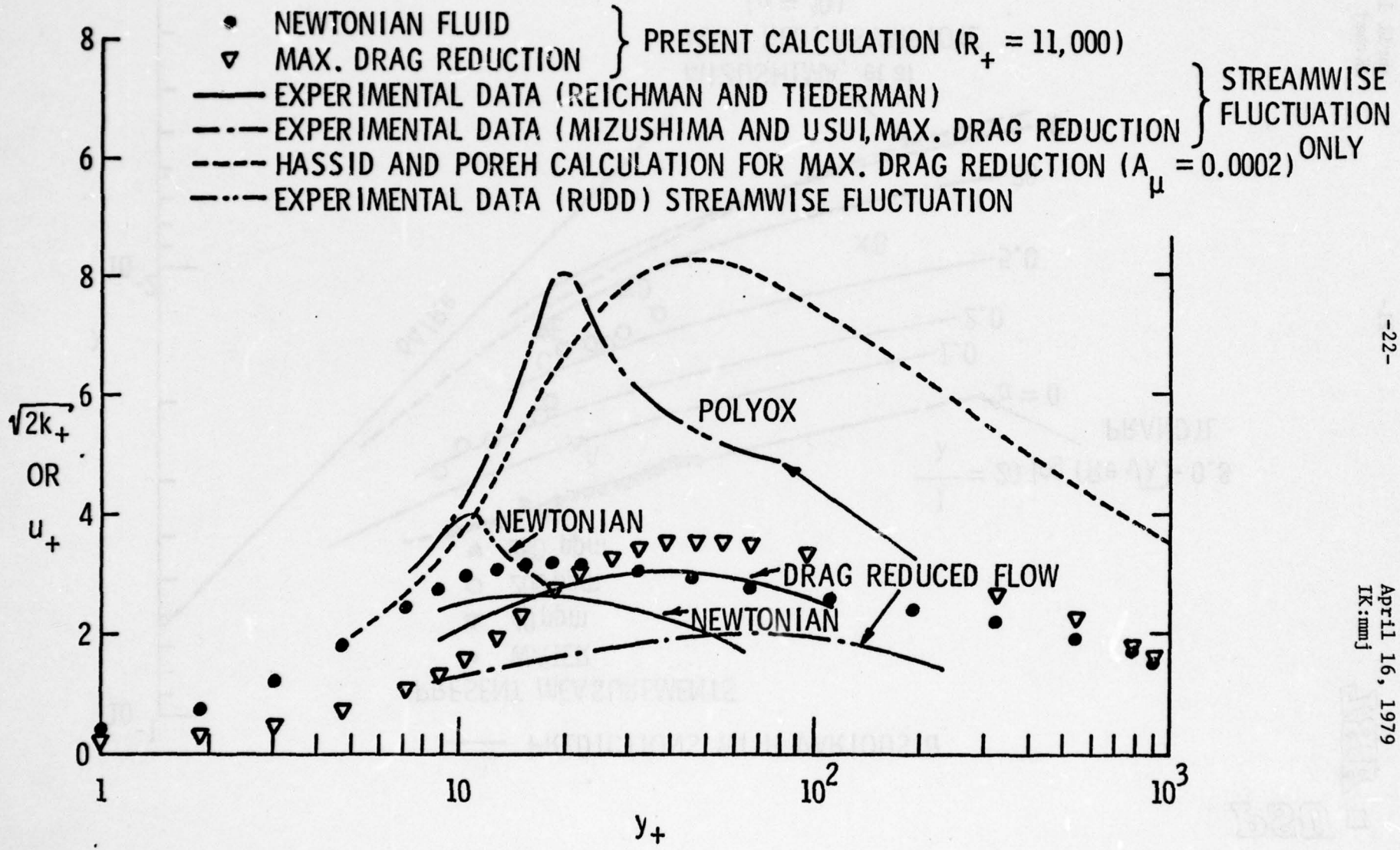

Figure 4. Turbulent Energy Distribution

April 16, 1979
IK:mmj

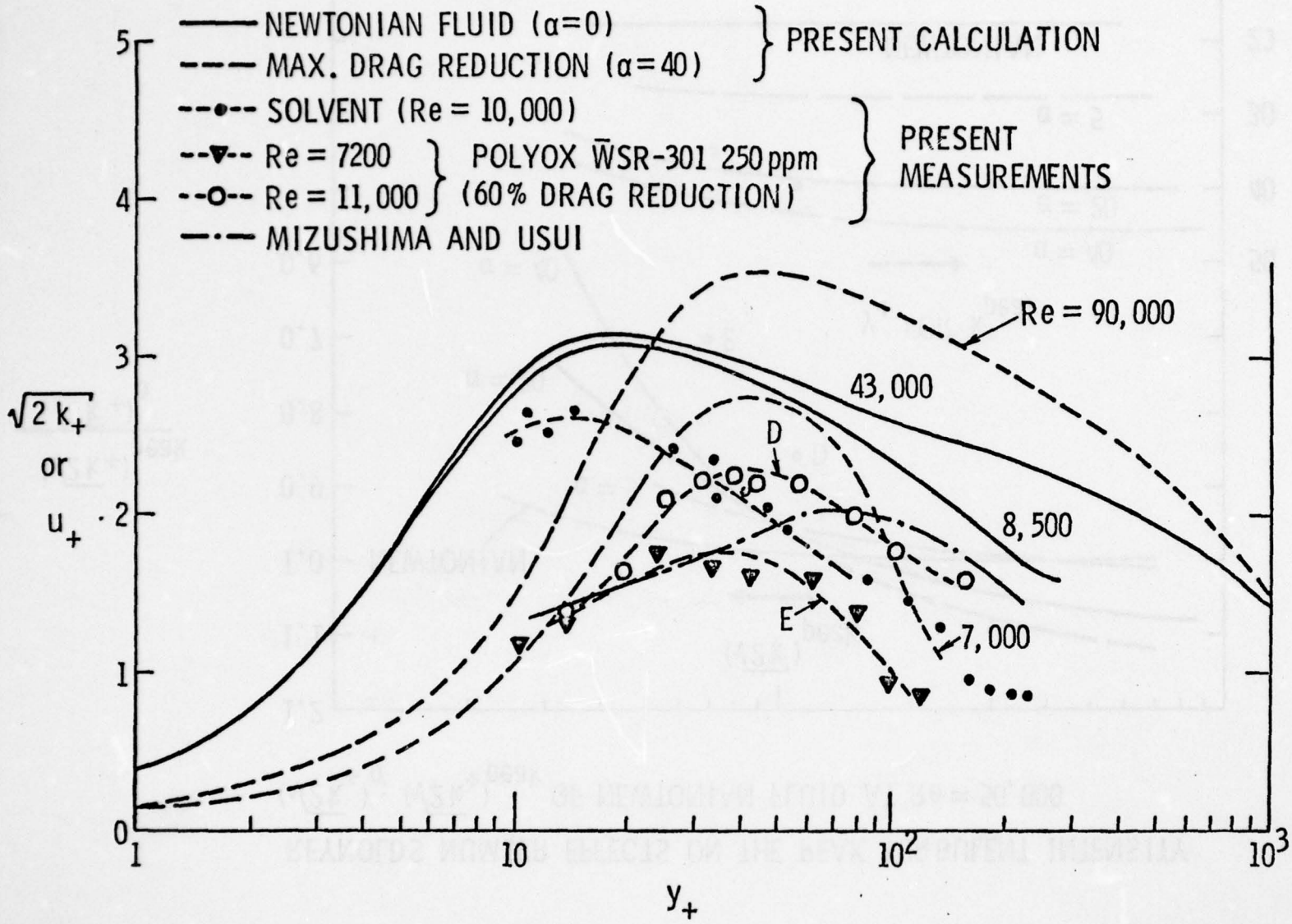

Figure 5. Turbulent Intensity Distribution

April 16, 1979
IK:mmj

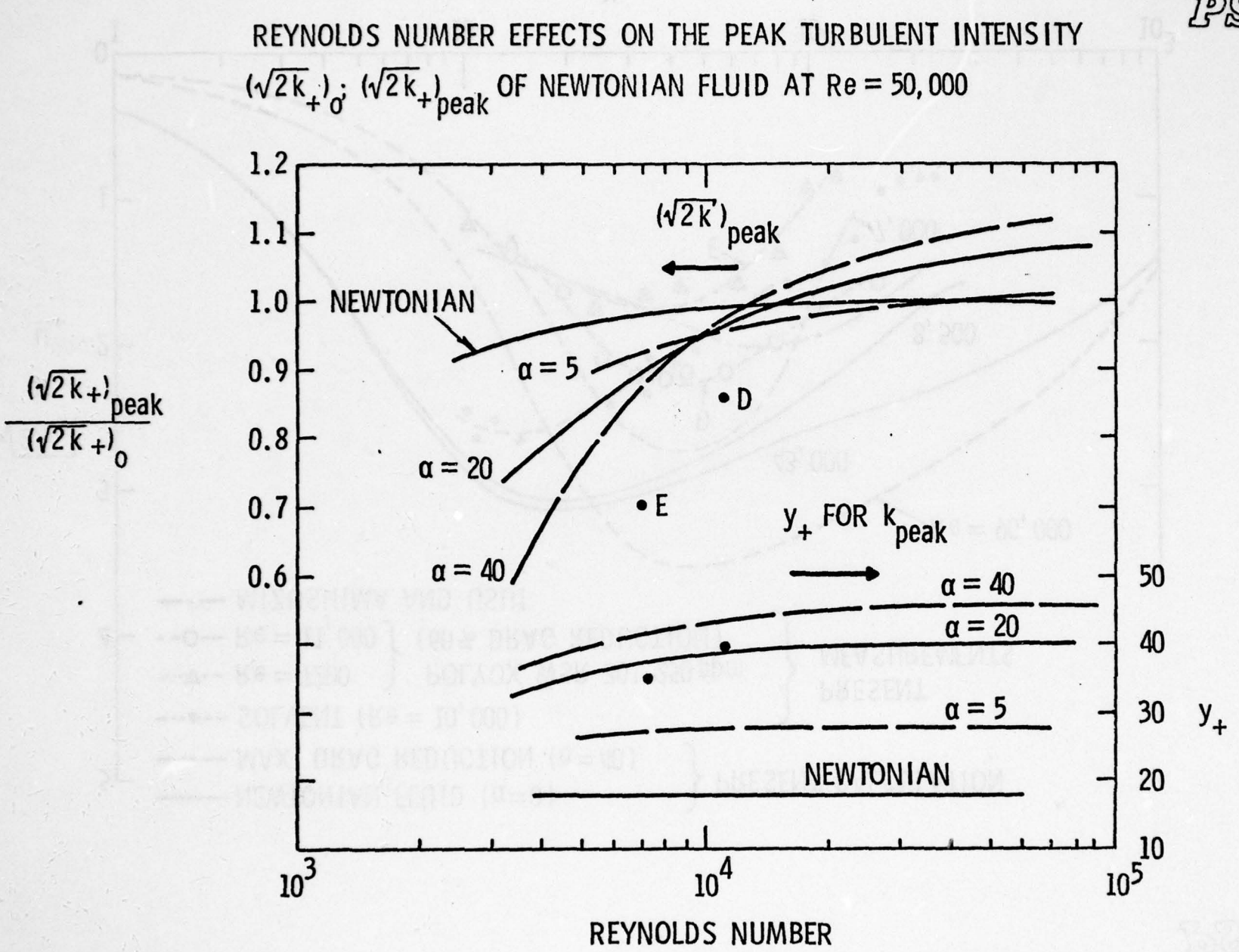

Figure 6. Reynolds Number Effects on the Peak Turbulent Intensity

April 16, 1979
IK:mmj

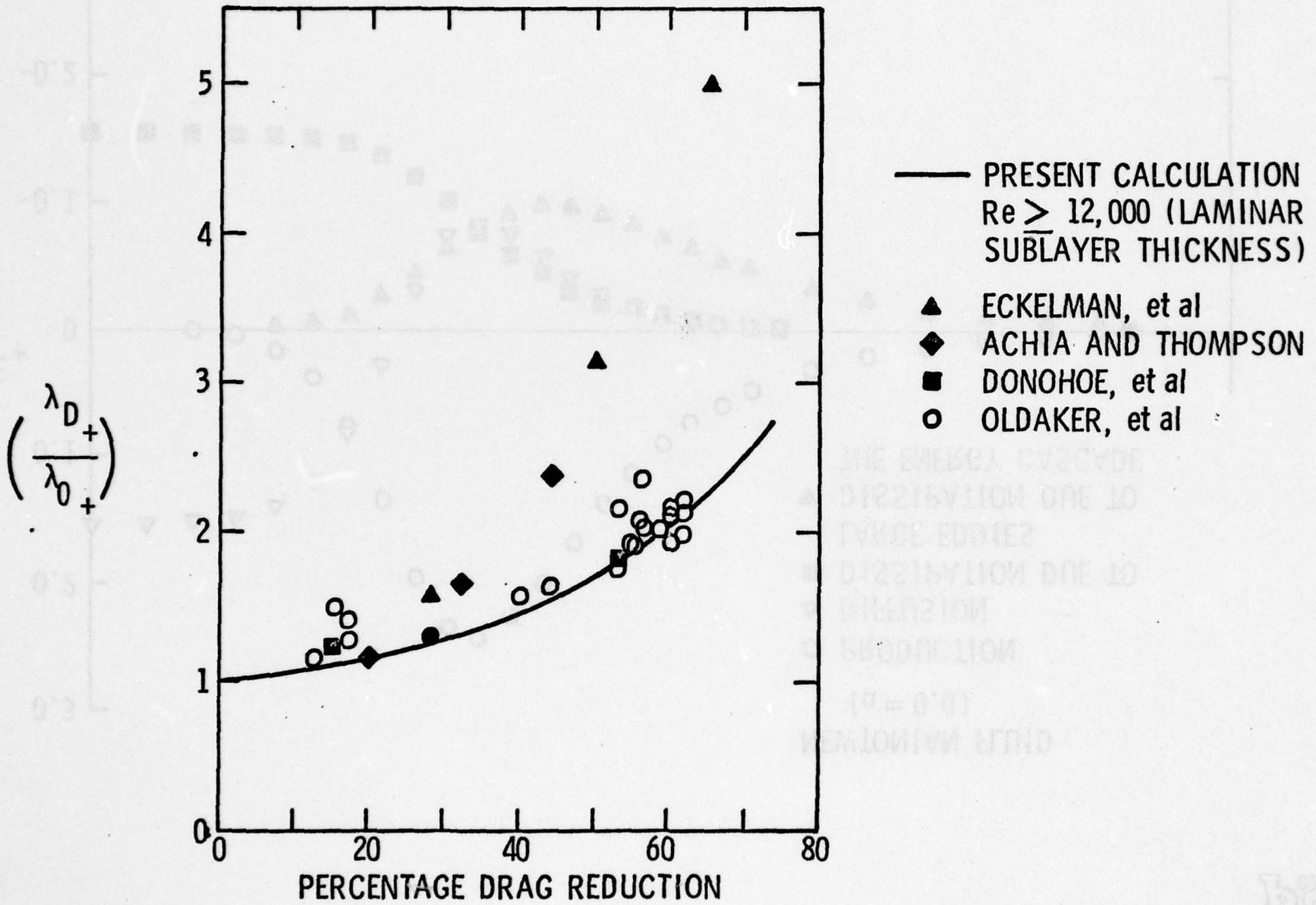

Figure 7. Calculated and Measured Changes in Length Scale

April 16, 1979
IK:mmj

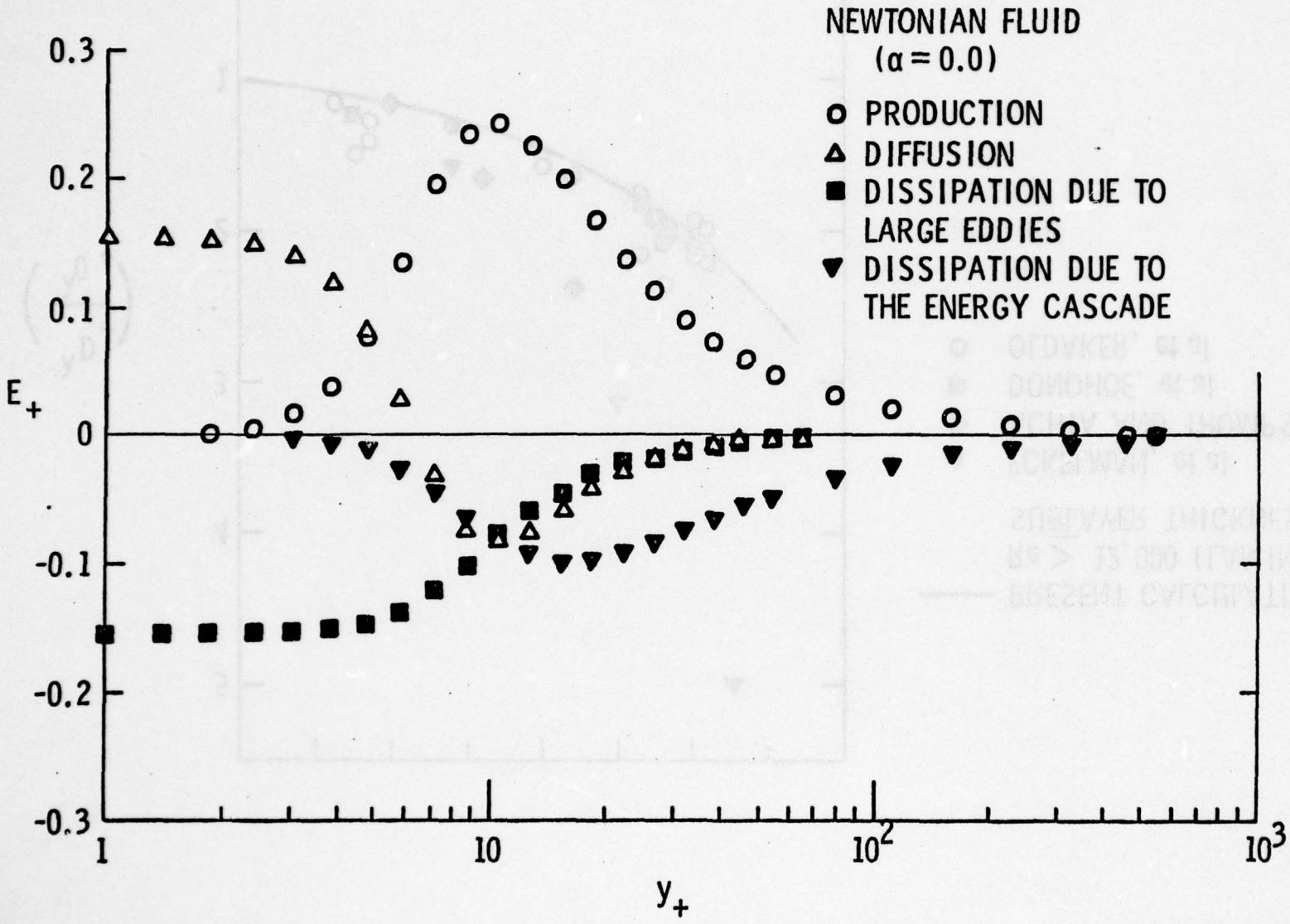

Figure 8. Turbulent Energy Balance (Newtonian Fluid)

April 16, 1979
IK:mmj

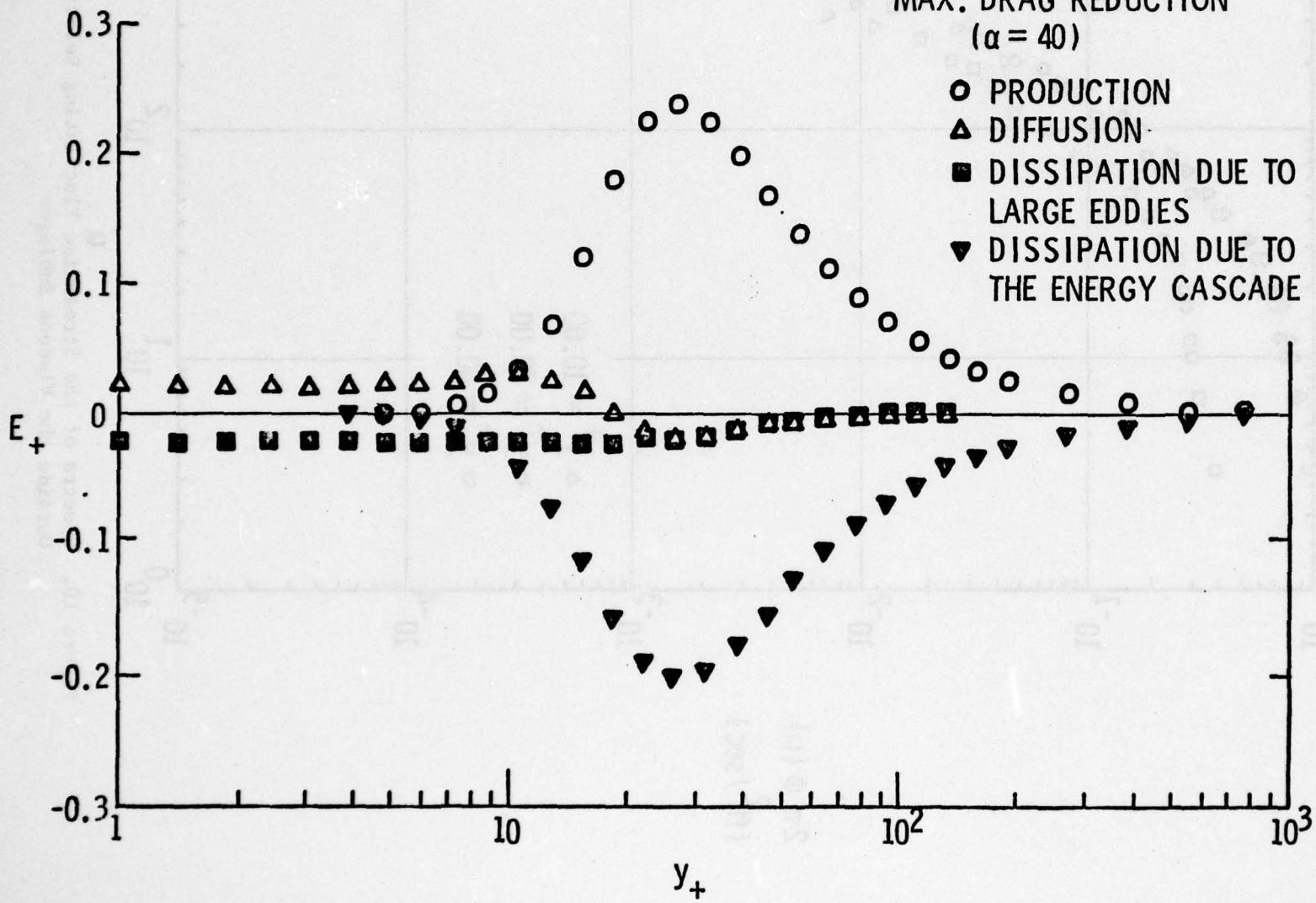

Figure 9. Turbulent Energy Balance (Polymer Solution)

April 16, 1979
IK:mmj

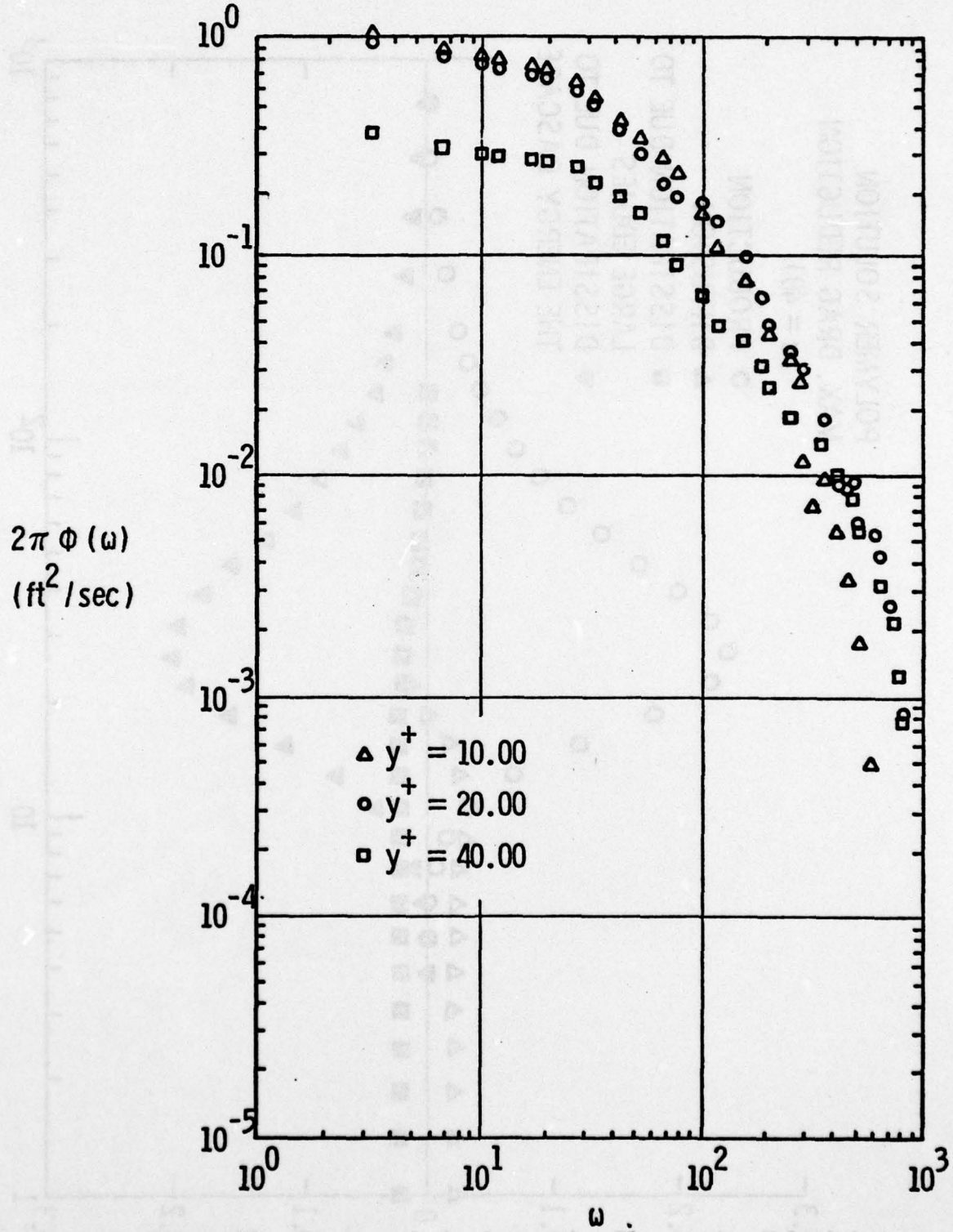

Figure 10. Spectra of the Streamwise Fluctuating Velocities Outside the Viscous Sublayer

DISTRIBUTION LIST FOR UNCLASSIFIED TM 79-66 by I. Kubo, dated April 16, 1979

Commander
Naval Sea Systems Command
Department of the Navy
Washington, DC 20362
Attn: Library
Code NSEA-09G32
(Copies No. 1 and 2)

Naval Sea Systems Command
Attn: S. M. Blazek
Code NSEA-05HB
(Copy No. 3)

Naval Sea Systems Command
Attn: J. G. Juergens
Code NSEA-05H
(Copy No. 4)

Naval Sea Systems Command
Attn: E. G. Liszka
Code NSEA-63R1
(Copy No. 5)

Naval Sea Systems Command
Attn: C. G. McGuigan
Code NSEA-63R2
(Copy No. 6)

Naval Sea Systems Command
Attn: T. E. Peirce
Code NSEA-63R3
(Copy No. 7)

Naval Sea Systems Command
Attn: A. R. Paladino
Code NSEA-05H1
(Copy No. 8)

Naval Sea Systems Command
Attn: G. Sorkin
Code NSEA-05R
(Copy No. 9)

Commanding Officer
Naval Underwater Systems Center
Newport, RI 02840
Attn: Library
Code 54
(Copy No. 10)

Naval Underwater Systems Center
Attn: D. Goodrich
Code 36315
(Copy No. 11)

Naval Underwater Systems Center
Attn: R. H. Nadolink
Code 36315
(Copy No. 12)

Naval Underwater Systems Center
Attn: C. N. Pryor
Code 01
(Copy No. 13)

Naval Underwater Systems Center
Attn: D. A. Quadrini
Code 36314
(Copy No. 14)

Naval Underwater Systems Center
Attn: R. Trainor
Code 36314
(Copy No. 15)

Naval Underwater Systems Center
Attn: F. White
Code 36314
(Copy No. 16)

Commanding Officer
Naval Ocean Systems Center
San Diego, CA 92152
Attn: D. Nelson
Code 6342
(Copy No. 17)

Naval Ocean Systems Center
Attn: M. M. Rieschman
Code 2542
(Copy No. 18)

Commander
David W. Taylor Naval Ship R&D Center
Department of the Navy
Bethesda, MD 20084
Attn: W. K. Blake
Code 1942
(Copy No. 19)

David W. Taylor Naval Ship R&D Center
Attn: J. H. McCarthy
Code 1552
(Copy No. 20)

David W. Taylor Naval Ship R&D Center
Attn: W. B. Morgan
Code 154
(Copy No. 21)

DISTRIBUTION LIST FOR UNCLASSIFIED TM 79-66 by I. Kubo, dated April 16, 1979

David W. Taylor Naval Ship R&D Center
Attn: M. M. Sevik
Code 19
(Copy No. 22)

Officer-In-Charge
David W. Taylor Naval Ship R&D Center
Department of the Navy
Annapolis Laboratory
Annapolis, MD 21402
Attn: J. G. Stricker
Code 2721
(Copy No. 23)

Commanding Officer
Naval Undersea Warfare Engineering Station
Department of the Navy
Keyport, WA 98345
(Copy No. 24)

Commander
Naval Surface Weapon Center
Silver Spring, MD 20910
Attn: J. L. Baldwin
Code WA-42
(Copy No. 25)

Naval Surface Weapon Center
Attn: G. C. Gaunaurd
Code R-31
(Copy No. 26)

Naval Surface Weapon Center
Attn: W. J. Glowacki
Code R-44
(Copy No. 27)

Office of Naval Research
Department of the Navy
800 N. Quincy Street
Arlington, VA 22217
Attn: R. D. Cooper
Code 438
(Copy No. 28)

Office of Naval Research
Attn: H. Fitzpatrick
Code 438
(Copy No. 29)

Defense Documentation Center
5010 Duke Street
Cameron Station
Alexandria, VA 22314
(Copies No. 30 - 42)

National Bureau of Standards
Aerodynamics Section
Washington, D. C. 20234
Attn: P. S. Klebanoff
(Copy No. 43)

Naval Research Laboratory
Washington, DC 20390
Attn: R. J. Hansen
(Copy No. 44)

NASA Lewis Research Center
21000 Brookpark Road
Cleveland, Ohio 44135
Attn: J. Adamczyk
MS 5-9
(Copy No. 45)

NASA Lewis Research Center
Attn: M. J. Hartmann
MS 5-9
(Copy No. 46)

NASA Lewis Research Center
Attn: W. M. McNally
MS 5-9
(Copy No. 47)

NASA Lewis Research Center
Attn: D. Morris
MS 60-3
(Copy No. 48)

NASA Lewis Research Center
Attn: N. C. Sanger
MS 5-9
(Copy No. 49)

Applied Physics Laboratory/
University of Washington (APL/UW)
1013 NE 40th Street
Seattle, WA 98105
(Copy No. 50)

Applied Research Laboratories/
University of Texas (ARL/UT)
Austin, Texas 78712
(Copy No. 51)

Dr. Bruce D. Cox
Stevens Institute of Technology
Davidson Laboratory
Castle Point Station
Hoboken, NJ 07030
(Copy No. 52)

DISTRIBUTION LIST FOR UNCLASSIFIED TM 79-66 by I. Kubo, dated April 16, 1979

California Institute of Technology
Jet Propulsion Laboratory
48000 Oak Grove Drive
Pasadena, CA 91109
Attn: Dr. L. Mack
(Copy No. 53)

Rand Corporation
1700 Main Street
Santa Monica, CA 90406
Attn: C. Gazley
(Copy No. 54)

Dr. Peter van Oossanen
Netherlands Ship Model Basin
Haagsteeg 2
P. O. Box 28
67 AA Wageningen
The Netherlands
(Copy No. 55)

Carl-Anders Johnsson
Statens Skeppsprovningsanstalt
Box 24001
S-400 22 Goteborg
Sweden
(Copy No. 56)

Dr. Ir. A. De Bruijn
Technisch Physische Dienst TNO-TH
Stieltjesweg 1
Postbus 155
Delft
The Netherlands
(Copy No. 57)

Dr. John Foxwell
Admiralty Research Laboratory
Teddington, Middlesex
England
(Copy No. 58)

Dr. Allen Moore
Admiralty Research Laboratory
Teddington, Middlesex
England
(Copy No. 59)

Professor R. E. Peacock
School of Mechanical Engineering
Cranfield Institute of Technology
Cranfield, Bedford MK430AL
England
(Copy No. 60)

Dr. Hans Mokelke
Mut-Munchen GMBLT
8 Munchen 50
Postfach 50 06 40
Germany
(Copy No. 61)

Professor J. P. Gostelow
School of Mechanical Engineering
NSW Institute of Technology
Broadway, Sidney
Austrailia
(Copy No. 62)

Dr. V. H. Arakeri
Department of Mechanical Engineering
Indian Institute of Science
Bangalore 560 012
India
(Copy No. 63)

Mr. Ken Ichirru
Hitachi Ltd.
4026 Kuji-cho
Hitachi-shi
Ibaraki-Ken, 319-12
Japan
(Copy No. 64)

Institute of High Speed Mechanics
Tohoku University
Sendai
Japan
(Copy No. 65)

Dr. Alan J. Acosta
California Institute of Technology
Division of Engineering for Applied Sciences
Pasadena, CA 91109
(Copy No. 66)

Dynamics Technology, Inc.
3838 Carson Street, Suite 110
Torrance, CA 90503
Attn: Wayne H. Haigh
(Copy No. 67)

Bolt, Beranek, and Newman
50 Moulton Street
Cambridge, MA 20136
Attn: Dr. N. A. Brown
(Copy No. 68)

DISTRIBUTION LIST FOR UNCLASSIFIED TM 79-66 by I. Kubo, dated April 16, 1979

Bolt, Beranek, and Newman
Attn: D. Chase
(Copy No. 69)

Bolt, Beranek, and Newman
Attn: K. L. Chandiramani
(Copy No. 70)

Dr. J. L. Lumley
Sibley School of Mechanical and
Aeronautical Engineering
Upson Hall
Cornell University
Ithaca, NY 14850
(Copy No. 71)

Calspan Corporation
4455 Genesse Street
Buffalo, NY 14221
Attn: Head Librarian
(Copy No. 72)

Dr. G. K. Sorovy
Mechanical Engineering Department
Iowa State University
Ames, Iowa 50010
(Copy No. 73)

Naval Postgraduate School
The Presidio
Monterey, CA 93940
Attn: Library
(Copy No. 74)

Iowa Institute of Hydraulic Research
The University of Iowa
Iowa City, Iowa 52240
(Copy No. 75)

Defense Advanced Research Projects Agency
1400 Wilson Boulevard
Arlington, VA 22209
Attn: P. Selwyn, TTO
(Copy No. 76)

Creare, Inc.
Box 71
Hanover, NH 03755
Attn: W. Swift
(Copy No. 77)

Rocketdyne Division
North American Aviation
6633 Canoga Avenue
Canoga Park, CA 91303
(Copy No. 78)

Aerojet General
Post Office Box 15847
Sacramento, CA 15813
(Copy No. 79)

Hydronautics, Inc.
Pindell School Road
Laurel, MD 20810
(Copy No. 80)

Dr. George F. Wislicenus
351 Golf Court (Oakmont)
Santa Rosa, CA 95405
(Copy No. 81)

Applied Research Laboratory
The Pennsylvania State University
Post Office Box 30
State College, PA 16801
Attn: G. H. Hoffman
(Copy No. 82)

Applied Research Laboratory
Attn: S. Deutsch
(Copy No. 83)

Applied Research Laboratory
Attn: J. J. Eisenhuth
(Copy No. 84)

Applied Research Laboratory
Attn: B. E. Robbins
(Copy No. 85)

Applied Research Laboratory
Attn: I. Kubo
(Copy No. 86)

Applied Research Laboratory
Attn: Garfield Thomas Water Tunnel Files
(Copy No. 87)